Heliyon 10 (2024) e35697

Contents lists available at ScienceDirect

Heliyon

journal homepage: www.cell.com/heliyon

Research article

Isolation of anti-tumor monoclonal antibodies targeting on MICA/B α3 domain by single B cell technology for colon cancer therapy

Xueyi Tang [a,1], Linhai He [a,1], Xiaoli Wang [b,1], Shuaichao Liu [b,c], Xiangning Liu [d], Xiaorui Shen [a], Yun Shu [a], Ke Yang [a], Qionghua Zhou [a], Zujian Shan [a], Yueming Wang [b], Changwen Wu [b], Zhenxing Jia [b], Tong Liu [b], Yayu Wang [b,*], Hua-Xin Liao [b,***], Yun Xia [a,**]

[a] *The People's Hospital of Xishuangbanna Dai Nationality Autonomous Prefecture, Xishuangbanna Dai Nationality Autonomous Prefecture, Yunnan, China*
[b] *Zhuhai Trinomab Pharmaceutical Co., Ltd, Zhuhai, Guangdong, China*
[c] *School of Life Sciences, University of Science and Technology of China, Hefei, Anhui, China*
[d] *Clinical Research Platform for Interdiscipline of Stomatology, The First Affiliated Hospital of Jinan University & Department of Stomatology, College of Stomatology, Jinan University, Guangzhou, China*

ARTICLE INFO

Keywords:
Colon cancer
MICA/B
Natural killer group 2D ligand
Immunotherapy
Natural killer group 2D receptor
Antibody screening technology
Single B cell PCR
NK cells
Immunosurveillance
Tumor escape

ABSTRACT

Colon cancer (CC) is one of the most common gastrointestinal malignancies. Effectiveness of the existing therapies is limited. Immunotherapy is a promising complementary treatment approach for CC. Major histocompatibility complex class I-related protein A and B (MICA/B) are ligands for NK cells. Shedding of MICA/B from the surface of tumor cells by cleavage of MICA/B at the membrane proxial region in MICA/B α3 structural domain is one of immune evasion strategies leading to escape of cancer cells from immunosurveillance. In this study, we generated a panel of MICA/B monoclonal antibodies (mAbs) and identified one of mAbs, mAb RDM028, that had high binding affinity to MICA/B and recognized a site on MICA/B α3 structural domain that is critically important for cleavage of MICA/B. Our study has further demonstrated that RDM028 augmented the surface expression of MICA/B on HCT-116 human CC cells by inhibiting the MICA/B shedding resulting in the enhanced cytotoxicity of NK cells against HCT-116 human CC cells and mediated anti-tumor activity in nude mouse model of colon cancer. These results indicate that mAb RDM028 could be explored for developing as an effective immuno therapy against CC by targeting the MICA/B α3 domain to promot immunosurveillance mediated by MICA/B-NKG2D interaction.

1. Introduction

Colorectal cancer (CC) is one of the most common cancers worldwide. In 2022, there were 151,030 new cases and 52,580 deaths of

* Corresponding author.
** Corresponding author.
*** Corresponding author.
E-mail addresses: wangyayu@trinomab.com (Y. Wang), larryhliao@trinomab.com (H.-X. Liao), xiayun69511@Sina.com (Y. Xia).
[1] All these authors contribute equally to this work.

https://doi.org/10.1016/j.heliyon.2024.e35697
Received 2 November 2023; Received in revised form 31 July 2024; Accepted 1 August 2024
Available online 3 August 2024

CC patients in the United States, accounting for 8.0 % and 8.6 % of the total number of cancer cases and deaths, respectively [1]. The high rate of metastasis and low rate of 5-year survival for patients with CC indicate that the current treatments in clinical care of CC are limited [2]. Comprehensive cancer treatments have achieved great progress, and targeted therapies have provided remarkable clinical benefits for patients with metastatic cancer [3–6]. Immunotherapy is a promising treatment modality that harnesses the innate immune system to selectively target cancer cells and holds tremendous potential for managing CC [2].

Natural killer group 2D receptor (NKG2D) is a type II transmembrane glycoprotein expressed on the surface of natural killer (NK) cells, natural killer T (NKT) cells, and T cells. The ligands for NKG2D include major histocompatibility complex class I-related chains A and B (MICA/B) and UL16-binding proteins (ULBPs) [7]. Interaction of NKG2D with its ligands leads to activation of antigen-specific cytotoxic T-lymphocyte-mediated cytotoxicity, NK cell responses, and cytokine production and plays an important role in cancer therapy by recognizing ligands on the surface of tumor cells and mediating the killing of tumor cells by NK cells [8]. MICA and MICB are highly homologous type I transmembrane proteins with three extracellular domains including α1 and α2 domains that interact with NKG2D, and α3 domain that is located close to the transmembrane domainin [9,10]. Expression of NKG2D ligands in healthy human tissues is low [11]. Thus, NKG2D-based effector populations target tumor tissues without affecting surrounding non-tumor tissues [12,13].

As an immune evasion strategy, MICA and MICB are proteolytically cleaved from the surface of tumor cells including CC cells [14] by enzymes such as endoplasmic reticulum protein 5 (ERp5) and matrix metalloproteinases (MMPs) [15,16] leading to escape of cancer cells from immune surveillance. Specific antibodies targeting the MICA/B α3 domain can inhibit the cleavage of MICA/B from the surface of tumor cells, and MICA immune complexes formed with α3-specific antibodies mediate killing of tumor cells by NK cells, indicating that MICA/B is a potential therapeutic target for cancers [9,17]. It has also been demonstrated that anti-MICA/B antibody had antitumor potential for human colorectal cancer cells *in vitro* study [18]. However, no reports on treatment of colon cancer with anti-MICA/B antibodies *in vivo* have been seen.

In this study, monoclonal antibodies (mAbs) that bind to the α3 structural domain of MICA and MICB were generated in BALB/c mice immunized with MICA/B proteins and isolated from flow-sorted single B cells of the immunized mice. Anti-tumor effects of these mAbs that bound to MICA/B were evaluated in anti-tumor cytotoxicity assays *in vitro* and *in vivo* in a nude mouse xenograft model of CC. We identified that one of mAbs, mAb RDM028, had high binding affinity to α3 domain of both MICA and MICB, mediated tumor killing in both *in vitro* and *in vivo* assays (Fig. 1). Thus, mAb RDM028 could be a potential antibody candidate for exploring the fesibility to be developed as an effective immuno therapy against CC by targeting the MICA/B α3 domain.

2. Materials and methods

2.1. Cell lines and culture

HCT-116 human CC cells were purchased from the American Type Culture Collection and cultured in RPMI-1640 basic medium (Life Technologies, USA) supplemented with 10 % fetal bovine serum (FBS) (Life Technologies), 1 % streptomycin and 1 % penicillin in a humidified incubator with 5 % CO_2 at 37 °C.

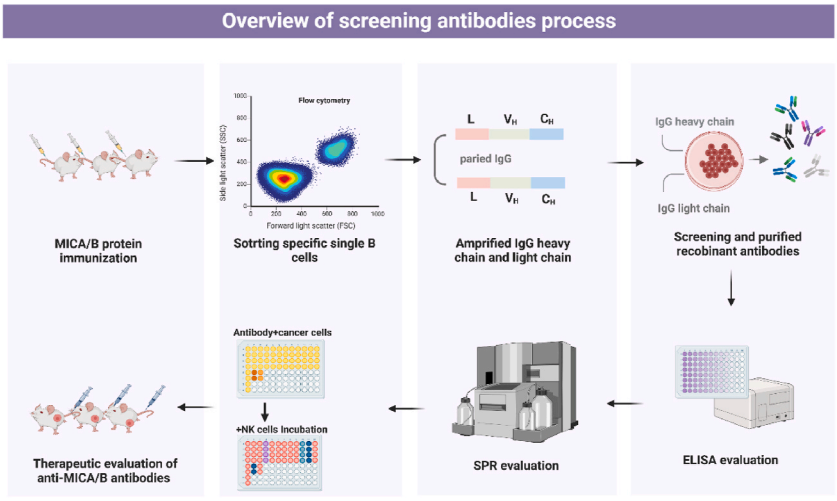

Fig. 1. Schematic representation of screening, characterization of monoclonal antibodies targeting major histocompatibility complex class I-related chains A and B, and the anti-tumor activity of these antibodies *in vitro* and *in vivo*.

2.2. Expression and purification of MICA, MICB, and respective α3 domains

Expression of gene constructs encoding MICA, MICB, MICA α3 domain or MICB α3 domain proteins containing the Avi-tag (GLNDIFEAQKIEWHE) for biotin labeling and 6-His tag for facilitating purification at the N terminus were designed, *de novo* synthesized and cloned into pCDNA3.1 mammalian expression plasmid (GenScript). Plasmid DNAs were purified from cultures using the PureLink HiPure Plasmid Maxiprep Kit (Thermo Fisher Scientific) and used for production recombinant proteins in 293F cells by transient transfection using polyethylenimine (Sigma-Aldrich). After 4 days of cell culture, recombinant proteins with His-tag were purified form supernatant of the transfected cell cultures using Ni-Charged MagBeads (GenScript) and stored at −80 °C till used.

2.3. Animal immunization for MICA/B antibodies

Three BALB/c mice were intramuscularly injected with an immunization mixture containing 25 μg each of MICA, MICB, MICA α3 domain and MICB α3 domain using QuickAntibody-Mouse2W (Biodragon) as adjuvant in a total volume of 100 μL per injection followed by three boost injections at 2-week intervals. Spleen and blood were harvested 7 days after the final immunization.

2.4. Detection of antibody titers in mouse serum by enzyme-linked immunosorbent assay (ELISA)

Purified MICA/B proteins were used to coat 96-well ELISA plates at 100 ng/100 μL per well in carbonate bicarbonate buffer (CBC) buffer, pH9.6. Plates were incubated at 4 °C overnight. Aliquots of 300μL/well of phosphate-buffer saline with 0.05 % Tween-20 buffer (PBST) containing 10 % sheep serum were added and incubated at 37 °C in humidified chamber for 2 h. The plates were washed three times with PBST buffer. Aliquots of 100 μL/well of 12 2-fold serial dilutions of the immunized mouse sera at the starting concentration of 1:50 in PBST buffer were added. The plates were incubated at 37 °C for 1 h followed by washing 3 times with PBST. Aliquots of 100 μL/well of horseradish peroxidase (HRP)-conjugated goat anti-mouse IgG (1:5,000) in PBST buffer were added. The plates were incubated at 37 °C for 1 h. After washing the plates five times with PBST, 100 μL/well of substrate 3,3′,5,5′-tetramethylbenzidine (TMB) (Solarbio) were added to the plates followed by incubation at room temperature for 5–10 min. The reaction was terminated with 50 μL/well of 2 M H_2SO_4. Absorbance was measured at 450–640 nm in ELISA reader. Antibodies in wells with absorbance at least four-fold greater than that of the negative control were judged as positive.

2.5. Sorting MICA/B antigen-specific B cells

A single-cell suspension of splenocytes was prepared by gently teasing of the harvested spleen from the mouse with the highest serum binding antibody titers and filtering through a cell strainer (BD Biosciences). The suspension was used for sorting single memory B cells by fluorescence-activated cell sorting. The splenocytes were washed once with RPMI 1640 medium (10 % FBS) and resuspended in 200 μL of PBS with 5 % FBS. Cells were incubated with the LIVE/DEAD Fixable Aqua Stain (Thermo Fisher Scientific), fluorescein isothiocyanate (FITC)-conjugated anti-mouse CD4 (BD Biosciences) and anti-mouse CD8a (BD Biosciences), allophycocyanin (APC)-conjugated anti-mouse CD45R (BD Biosciences), phycoerythrin (PE)-conjugated IgD (BD Biosciences), BV650-conjugated anti-mouse IgG (BD Biosciences), PE-Cy7-and BV421-conjugated MICA/B antigens for identifying antigen-specific memory B cells. Cells were incubated with antibodies for 30 min at room temperature in the dark. Cells were washed twice with PBS containing 5 % FBS and resuspended in 3 mL of PBS containing 5 % FBS. After filtered through a 200-mesh strainer to remove cell clumps, single-cell suspension was subjected for sorting single memory B cells using the FACSMelody™ Cell Sorter (BD Biosciences). Lymphocytes were gated by FSC-A/SSC-A dot plot, where FSC-A and SSC-A are the areas of the forward and side scatter pulse. Live cells were gated by using the Aqua Stain. MICA/B antigen-specific memory B cells with $CD4^-/CD8a^-/CD45R^+/IgG^+/IgD^-$ as well as PE-$Cy7^+$ and $BV421^+$ dual positive were gated and sorted as single cells into 96-well plates containing reverse transcriptase buffer and stored at −80 °C. Data were analyzed using FlowJo software.

2.6. Isolation of immunoglobin (Ig) variable region genes by RT/PCR

cDNAs from single B cells in the individual wells in 96-well plates were prepared using Superscript IV reverse transcriptase (Thermo Fisher) with specific reverse transcription primers. Mouse antibody variable-region genes were amplified by two rounds of PCR using AmpliTaq Gold 360 Master Mix DNA polymerase. As most of mouse B cell surface Ig genes have κ light chains [19], light primers used in our study only included primers for amplifying κ light chains. The first round of nested PCR contained the forward primers derived from the Ig gene leader sequences of the variable region genes of the heavy- (V_H) and light-chain (V_L) and the reverse primers derived from the Ig constant regions of heavy- and κ light-chain. The second round PCR used forward primers designed to overlap the sequence tag in the first round PCR products for the new round of PCR amplification. In the second round, reverse primers were designed to target mouse antibody constant CH1/CL1 genes tailed with the mouse antibody constant gene IgG2a (CH) or Ig κ (CL). PCR products were sequenced for Ig gene annotation and used to generate expression constructs for producing recombinant antibodies.

2.7. Constructing recombinant mouse Ig gene expression cassettes using overlapping PCR

The amplified V_H and V_K genes were used to assemble the linear expression constructs for production of recombinant antibodies by overlapping PCR as previously described [20]. The forward overlapping DNA fragment containing CMV promoter with DNA sequence

overlapping with the tag sequence in the 5′ end of the amplified PCR products of the isolated V_H and V_K genes. The reverse overlapping DNA fragment comprised of a mouse IgG2a constant domain (330 aa, GenBank Accession No. V00798.1) or mouse Igκ light-chain constant domain (107 aa, GenBank Accession No. V00802.1) with DNA sequences overlapping with the tag sequence in the 3' of the isolated V_H or V_K PCR products. The resulting linear full-length mouse IgG2a and Igκ gene expression constructs generated by the overlapping PCR were purified using the QIAquick PCR Purification Kit (Qiagen, Valencia, CA) and used for transfection.

2.8. Production of recombinant mAbs

To produce small quantities of recombinant antibodies for initial screening, HEK 293T cells cultured at 80–90 % confluence in 12-well tissue culture plates (Becton Dickson, Franklin Lakes, NJ) were used. Cells in 12-well tissue culture plates were co-transfected with the purified Ig V_H (1 μg) and V_K gene expression cassettes using PolyFect (Qiagen, Valencia, CA). The transfected cells were cultured in RPMI-1640 basic medium (Life Technologies, USA) supplemented with 2 % fetal bovine serum (FBS) (Life Technologies), 1 % streptomycin and 1 % penicillin in a humidified incubator with 5 % CO2 at 37 °C for 3 days. Supernatant of the transfected cultures were harvested and used directly for screening MICA/B- specific mAbs.

For production of purified full-length IgG antibodies, the isolated V_H and V_K genes were cloned into pCDNA3.1+ (Invitrogen) mammalian expression vector containing either mouse IgG2a constant region gene or the mouse kappa light-chain constant region gene using standard recombinant DNA technology. To produce chimeric antibody with human IgG1 heavy chain constant domain region, The Ig heavy-chain expression construct with the constant region of mouse IgG2a was replaced with the constant region gene of human IgG1. Antibodies were also produced in HEK 293T cells by transfection using polyethylenimine (Sigma-Aldrich). After 4 days of culture, recombinant antibodies were purified form supernatant of the transfected cell cultures using Protein A beads (GenScript).

2.9. Screening for antibodies binding to α3 domain proteins by ELISA

Antibodies in the supernatant harvested from the transfected 293T cell cultures were screened for the ability to bind MICA, MICB, and their respective α3 domain proteins by ELISA as described previously [21]. Briefly, proteins were coated to 96-well high-binding ELISA plates (Nunc) (100 ng/well) in CBC buffer, pH 9.6. The plates were kept at 4 °C overnight, blocked with goat serum for 2 h at room temperature followed by washing 3 times with PBST, incubated with the supernatants of the transfected 293T cell cultures at 37 °C for 1 h, and then incubated with goat anti-mouse HRP-conjugated IgG (1:10000) (Promega) diluted in blocking buffer at 37 °C for 1 h. The plates were washed five times with PBST followed by addition of 100 μL of TMB to each well. The reaction was terminated using 2 M H_2SO_4 (50 ml per well). Absorbance was measured at 450–640 nm using a microplate reader. The half-maximal effective concentrations (EC_{50}) of mAbs were determined by curve fitting using GraphPad Prism.

2.10. SDS-PAGE and western blotting

Produced recombinant antibodies were analyzed by SSD-PAGE and Western blots. Proteins were loaded at 1.0 μg per lane for Coomassie blue staining and 0.2 μg per lane for Western blotting and were fractionated on 4–12 % Bis-Tris SDS-PAGE gels (GenScript) by running under reducing and non-reducing conditions at 200 V for 30 min. For Western blots, proteins were transferred to nitro-cellulose membranes. Membranes were probed with goat anti-mouse alkaline phosphatase-conjugated IgG [heavy and light chain],1:3000; Promega). Immunoblots were visualized using Western Blue substrate (Promega).

2.11. Binding kinetics measured by surface plasmon resonance (SPR)

Binding kinetics were measured by SPR using Biacore 8K (GE Healthcare). Running buffer in all experiments was HBS-EP (10 mM HEPES pH 7.4, 150 mM NaCl, 3 mM EDTA, 0.005 % surfactant P20). Anti-MICA/B antibodies were injected into channel at room temperature and captured by protein A immobilized on a sensor chip (GE Healthcare). Subsequently, aliquots of MICA or MICB at different concentrations were injected into the channel at flow rate of 40 μL/min for binding time of 90 s (s), and dissociation time of 5–10 min. Chip surfaces were regenerated after each cycle using 10 mM glycine pH 1.5 at a flow rate of 30 μL/min and a regeneration time of 90 s. Predetermined concentrations of antibodies, MICA and MICB were utilized to achieve appropriate corresponding response unit (RU) values.

2.12. Cluster of antibodies by cross competitive binding assays

Binding relationship of the isolated mAbs to MICA and MICB was assessed by SPR using a Biacore 8K instrument. MICA at concentration of 100 nM or MICB protein at concentration of 500 nM in HBS-EP was captured using a His-tag sensor chip (GE Healthcare) at room temperature by injection into the chanel with flow rate of 10 μL/min for binding time of 60 s. Anti-MICA/B antibodies were tested for cross reactivity by 2 injections. The tested antibodies were first injected and flowed over the MICA or MICB protein captured on the chips. Binding curves (reflected as RU) of the tested antibodies to MICA or MICB protein were measured over time. The same or different antibody was injected the second time and flowed over the surface. All antibodies were tested at a saturating concentration of 300 nM except for RDM044 at 1000 nM. The binding time was 180 s, the flow rate was 10 μL/min, and the dissociation time was 30 s. Chip regeneration was performed using 10 mM glycine pH 1.5.

2.13. Surface expression of MICA/B analyzed by flow cytometry

HCT-116 human CC cells were seeded in 6-well plates at a density of 1.2×10^6 cells per well and cultured in RPMI-1640 medium supplemented with 10 % FBS, 1 % streptomycin and 1 % penicillin in a humidified incubator with 5 % CO_2 at 37 °C. Anti-MICA/B antibodies at concentrations ranging from 0.01 nM to 100 nM were added to the individual wells in duplicates for each concentration of antibodies. Cells were incubated at 37 °C for 24 h. Then, cells from the individual wells were first detached using non-tripsin Versene Cell Dissociation Solution (Gibco), resuspended in test tubes in 100 μL per original well of cells with sterile PBS containing 2 % FBS and incubated with 3 μL of Human TruStain FcX (Biolegend) for 10 min on ice to block the Fc receptors on the cell surface. Two microliters of commerically available APC-conjugated anti-MICA and MICB α3 domain human antibody (Biolegend) were added and incubated for 30 min on ice. Mean fluorescence intensity (MFI) reflecting the cell surface expression of MICA/B on cells was measured by flow cytometry, and data were analyzed using FlowJo software version 10.8.1.

2.14. Effect of anti-MICA/B antibodies on shedding of MICA/B from cells

HCT-116 human CC cells were cultured in RPMI-1640 medium (Gibco) supplemented with 10 % FBS, 1 % streptomycin and 1 % penicillin. Cells were seeded in 6-well plates at a density of 1.2×10^6 cells per well. Anti-MICA/B antibodies at 5 different concentrations ranging from 0.01 nM to 100 nM were added to individual wells (two replicates per group) to test the effect of antibodies on the shedding of MICA/B proteoin from HCT-116 human CC cells. The plates were cultured for 48 h in a 5 % CO_2 and at 37 °C incubator. The cell cultures were subjected to centrifugation at $1000 \times g$ for 10 min to collect the culture supernatants for testing the MICA/B protein in the medium by using the Human MICA DuoSet ELISA kit (R&D system) and cells for analyzing the surface expression of MICA/B by flow cytometry.

2.15. Isolation of human NK cells

Peripheral blood samples were obtained from healthy volunteers, and peripheral blood mononuclear cells (PBMCs) were isolated by Ficoll-Paque PLUS (GE Healthcare) density gradient centrifugation. Cells were washed with sterile PBS and incubated with the LIVE/DEAD Fixable Aqua Stain (Thermo Fisher Scientific) and fluorescent dye labeled antibodies against CD3 and CD56 for 30 min in the dark. Cells were washed with PBS and transferred to sample tubes. $CD3^{-}CD56^{+}$ cells were sorted and collected by flow cytometry. Sorted cells were resuspended in RPMI 1640 medium supplemented with 10 % FBS, 1 % streptomycin and 1 % penicillin. Cells (1.0×10^6 per mL) were transferred to 24-well plates supplemented with recombinant human interleukin 2 (1000 U/mL) (Pepro Tech) to activate NK cells and incubated in an incubator with 5 % CO_2 at 37 °C for 24 h.

2.16. Cytotoxicity assays

Cytotoxicity assays were carried out by using the CytoTox 96 non-radioactive cytotoxicity assay kit (Promega). In brief, HCT-116 cells as target cells were seeded in 6-well plates at a density of 1.2×10^6 cells per well and treated with either RDM028 antibody, RDM028hG1 chimeric antibody or a negative control antibody at the final concentrations of 20 μg/mL. The plates were kept in an incubator with 5 % CO_2 at 37 °C for 24 h to suppress MICA/B protein release from the cell surface. The treated cells were detached from culture dishes using Versene (Gibco) and seeded with NK cells at a ratio of 1:10 in two 96-well round bottom plates.

To confirm that the effect of anti-tumor cytotoxicity promoted by RDM028 antibody was indeed mediated through the intereation of MICA/B with NKG2D receptor, in addition to supplementing with anti-MICA/B antibodies (20 μg/mL), another set of cultures was supplemented with a known MICA/B receptor blocking antibody 1D11 (BioLegend) at 20 μg/mL.

Controls, including total maximum and spontaneous lactate dehydrogenase (LDH) release from target cells, spontaneous LDH release from NK cells, culture medium background, and volume calibration, were established to ensure the measurement accuracy. The plates were centrifuged at 250*g* for 4 min and kept in a humidified incubator with 5 % CO_2 at 37 °C for 6 h. Then, 45 min before supernatant collection, aliquots of 10 μL/well of lysis solution (10 ×) were added to two control wells (volume calibration and maximum LDH release from target cells) to completely lyse the target cells. The plates were centrifuged at 250*g* for 4 min at room temperature, and 50 μL of the supernatant was transferred to another 96-well plate. To each well, 50 μL of a newly configured Substrate Mix was added and incubated for 30 min at room temperature under light-proof conditions. Finally, the reaction was interrupted using 50 μL of stop solution, and absorbance was measured at 490 nm using a microplate reader (Bio Tek, USA). Cytotoxicity was calculated according to the following equation:

$$\%\ \text{Cell toxicity} = \frac{\text{Experimental group - spontaneous LDH release from effector cells - spontaneous LDH release from target cells}}{\text{maximum LDH release from target cells - spontaneous LDH release from target cells}}$$

Experimental group: absorbance of all experimental wells minus absorbance of control wells.

Spontaneous LDH release from effector cells: absorbance of the standard concentration of LDH released by NK cells minus absorbance of the control medium.

Spontaneous LDH release by target cells: absorbance of the standard concentration of LDH released by target cells minus absorbance of the control medium.

Maximum LDH release by target cells: absorbance of the maximum concentration of LDH released by target cells minus absorbance

of the control medium.

2.17. Anti-tumor effect of MICA/B-reactive antibody measured in nude mouse model

Five-week-old female BALB/c nude mice were purchased from the Zhuhai BesTest Bio-Tech Co. Ltd. HCT-116 cells (5.0×10^6) in 100 μL PBS per mouse were injected subcutaneously into the right flanks of mice. At 48 h after inoculation, mice were randomly assigned to receive either 200 μg of RDM028hG1 or the same volume of PBS on days 1, 3, 7 and 14. Tumor volume (mm^3) was measured and calculated using the formula (tumor length × tumor width^2) × 0.5. Mice were sacrificed when the tumor volume reached 2000 mm^3.

2.18. Statistics

Comparisons of quantitative data between different groups were conducted using two-way ANOVA formula. Statistical analysis was performed using GraphPad Prism 6.0 (GraphPad Software Inc, San Diego, CA, USA) software. $P < 0.05$ was considered statistically significant.

3. Results

3.1. Isolation of anti-MICA/B antibodies by single B cell sorting

We designed and expressed soluble recombinant MICA/B and MICA/B α3 domain proteins for mouse immunization (Fig. 2A) and characterization of the isolated mAbs. Mice were immunized four times, and spleenocytes were extracted from the spleen. A stepwise gating strategy was employed to isolate memory B cells with high specificity for MICA/B (Fig. 2B). This approach enabled the identification of B cells with the surface receptor bound specifically by the fluorescen-labeled MICA/B proteins. As most of mouse B cell surface Ig have κ light chains [19], we used primers for only κ light chains in combination with the primers for heavy chains in reverse

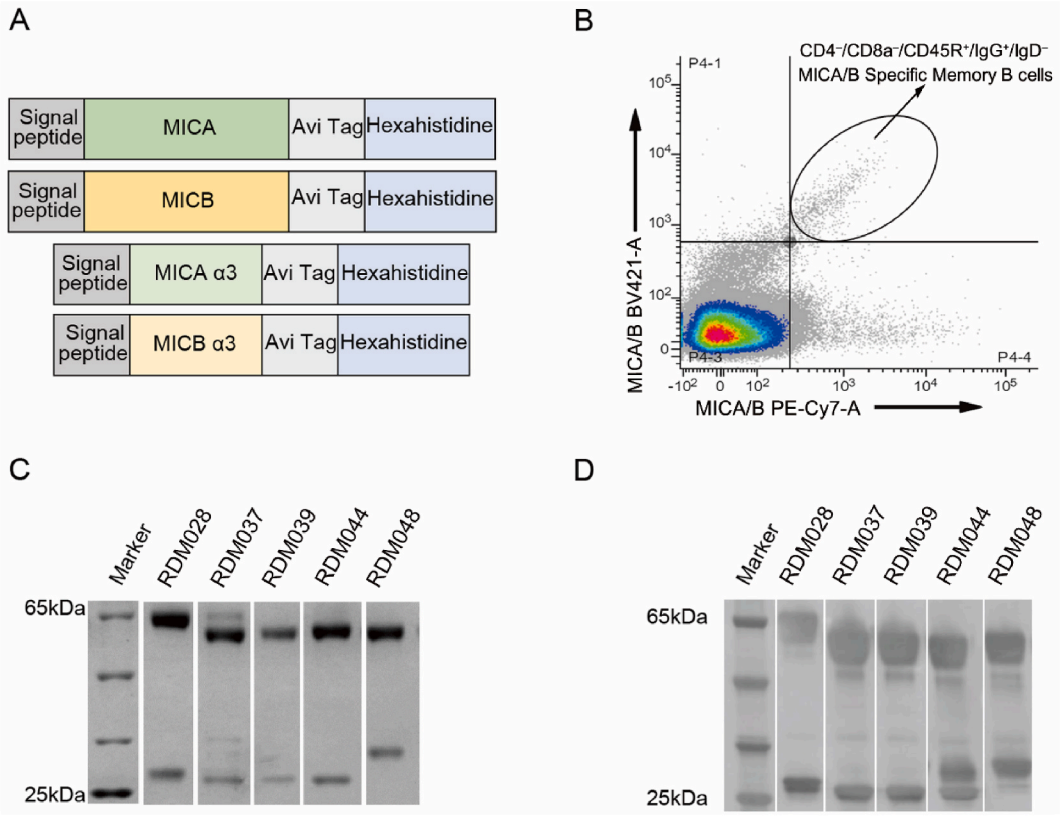

Fig. 2. Expression constructs of MIC proteins, flow sorting antigen-specific memory B cells and selected mAbs. Expression constructs of MIC A, MIC B, MIC A α3 and MIC B α3 proteins with the N terminal tags of AVI for biotin labeling and His-6 for facilitating purification (A). Flow sorting antigen-specific B cells gated using the strategy as indicated in the upper right quardrant identified by BV421-labeld (y axis) and PE-Cy7-labeled (x axis) MIC A/B proteins (B). SDS-PAGE (C) and Western blot analysis (D) of the purified mAbs idicated on top of the gels.

transcription polymerase chain reaction (RT-PCR) to isolate Ig variable heavy- and κ light-chain (V_H and V_K) gene segments from the sorted MICA/B-specific B cells. After RT reaction, two-round nested PCRs were conducted. Total of 66 pairs of V_H and V_K genes were isolated and used to assemble the full-length Ig heavy- and ligh-chain gene expression constructs to produce recombinant mAbs in 293T cells by transient transfection. The ability of mAbs to bind MICA and MICB proteins was first screened by ELISA. A total of 18 recombinant antibodies were identified to react with recombinant MICA/B proteins (Supplementary Table 1). Five mAbs, RDM028, RDM037, RDM039, RDM044 and RDM048, with the ability to bind strongly to MICA/B proteins were selected for production of purified mAbs for further characterization (Supplementary Table 1). The purified antibodies were evaluated in quality control by SDS-PAGE and western blotting (Fig. 2C and D and Supplementary Fig. 1).

4. Binding specificity and affinity of mAbs to MICA/B

Binding specificity of all five purified mAbs was first tested to bind the full-length MICA/B proteins by ELISA (Fig. 3A and B; Supplementary Table 2). We found that RDM028, RDM037, RDM039, RDM044 and RDM048) all bound MICB with EC_{50} of 0.002900, 0.01607, 0.01027, 0.003913 and 0.01398 μg/mL, respectively (Fig. 3A). Except RDM039, the other 4 mAbs, RDM028, RDM037, RDM044 and RDM048, also bound to MICA with EC_{50} values of 0.002569, 0.02642, 0.003929 and 0.01976 μg/mL, respectively (Fig. 3B). Next, we evaluated whether these mAbs could bind to the more defined α3 domain of both MICA and MICB by ELISA (Fig. 3B and A; Supplementary Table 2). We found that except RDM044, the other 4 mAbs, RDM028, RDM037, RDM039 and RDM048 bound MICB α3 with EC_{50} of 0.003711, 0.1071, 0.009013 and 0.02371 μg/mL, respectively. However, only RDM028 bound strongly with MICA α3 with EC_{50} of 0.04688, and RDM048 and RDM037 bound MICA α3 weakly with EC_{50} of 1.604 and 0.4681 μg/mL, respectively, while the other 2 mAbs did not bind MICA α3.

Furthermore, we assessed the binding affinity of these mAbs to MICA and MICB by SPR. The K_D values of RDM028, RDM037, RDM044 and RDM048 binding to MICA were 2.14, 23.4, 62.8 and 184 nM, respectively (Fig. 3C; Supplemental Table 3). The binding affinity of these antibodies to MICB was 2.84, 31.6, 34.6 and 212 nM, respectively. RDM039 bound to MICB (K_D of 187 nM) but not to MICA (Fig. 3D; Supplemental Table 3). These results were also consistent with ELISA results.

4.1. Cross reactivity of MICA/B binding mAbs

Since ELISA results indicated that RDM028, RDM037 and RDM048 bound to the α3 domains of MICA and MICB, cross reactivity of these 3 mAbs was evaluated by cross competitive binding assays by SPR (Fig. 4A). We found that RDM028 and RDM037 almost completely blocked each other for binding to both MICA (Fig. 4B) and MICB (Fig. 4C) suggesting that these 2 antibodies recognize the same or similar antigenic epitope located in the MICA α3 domain (Fig. 4D). In contrast, RDM044 and RDM048 did not block each other from binding to either MICA (Supplementary Fig. 2A) and MICB (Supplementary Fig. 2B) indicating that these two antibodies targeting distinct sites in MICA (Fig. 4D).

4.2. Ability of MICA/B-reactive antibodies to augment surface expression of MICA/B

All 5 mAbs were tested for the role in the surface expression of MICA/B protein in HCT-116 cells. We found that RDM028 among the

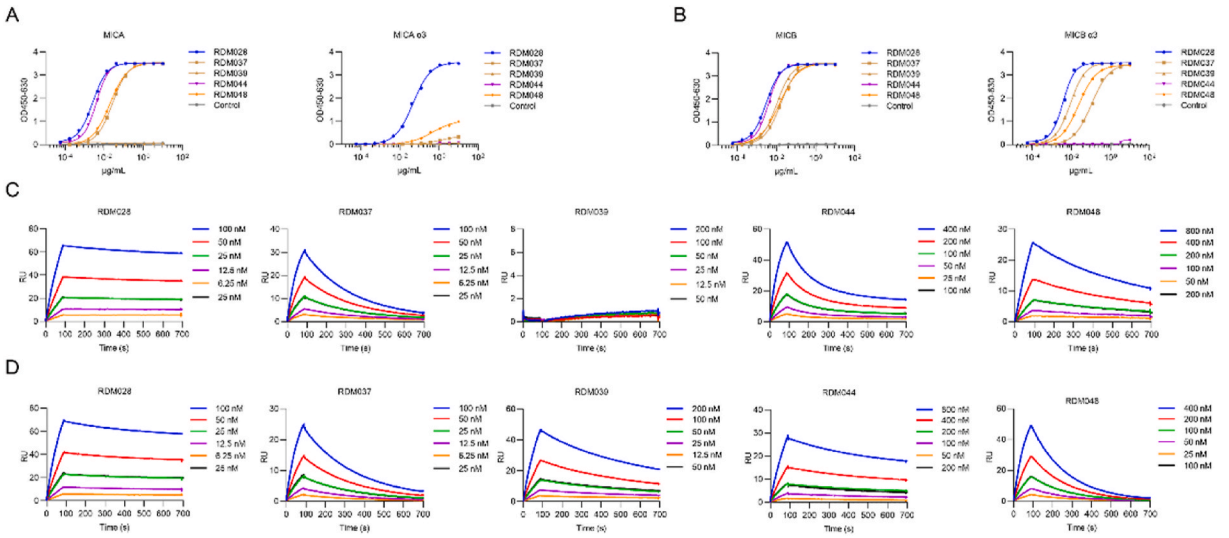

Fig. 3. Specificity and binding affinity of mAbs to MICA/B. Binding of the individual mAbs at the indicated concentrations to MICB (A), MICA (B), MICB α3 structural domain (A) and MICBA α3 structural domain (B) in ELISA assys. Binding kinetics of the indicated mAbs to MICA (C) and MICB (D) were measured by SPR.

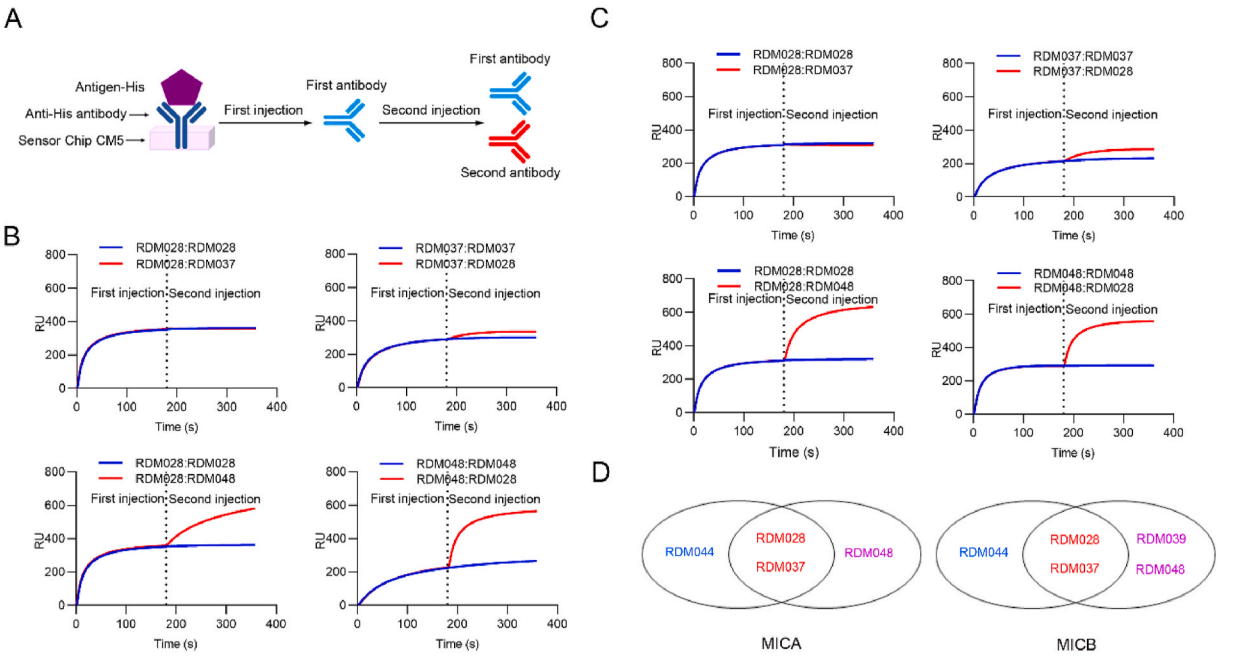

Fig. 4. Cross-reactivity of mAbs analyzed by cross competitive binding assays by SPR. Cross competitive blocking of 3 α3 domain-reactive antibodies as indicated on the individual plots was assessed by SPR as illustrated schematically above the top of the plots (A). Recombinant MICA (B) and MICB (C) were captured using anti-His tag antibody immobilized on the CM5 sensor chip. Each plot corresponds to the binding curve of an antibody to MICA or MICAB in response units (RU) on the y-axis over time of seconds on the x-axis. The same antibody (blue curves) or different antibodies (red curves) were allowed to interact with MICA or MICB coupled to the CM5 sensor chip by injection at two time points (0 and 200 s). MAbs RDM028, RDM037 and RDM048 were clustered based on their ability to compete for binding to MICA and MICB (D).

5 mAbs tested had the strongest ability to augment the surface expression of MICA and MICB proteins on HCT-116 cells (Fig. 5A). Therefore, RDM028 was selected for further studies. As the first step toward a long-term goal to humanize RDM028 in our hope that it can eventually be developed as an anti-tumor therapeutic agent, the original mouse heavy-chian constant region of RDM028 was replaced with the constant region of human IgG1 to produce the chimeric RDM028hG1 antibody. Compared to the original RDM028 (Supplemental Table 3), binding profiles of the chimeric RDM028hG1 to MICA and MICB as well as their respective α3 domains were similar (Fig. 5B and C; Supplemental Tables 4 and 5).

It has been shown that MICA/B on the surface of cancer cells can be shed from the cell surface by cleavage at the membrane-proximal region in MICA and MICB α3 domain [15,22]. We assessed whether binding of RDM028hG1 to MICA/B could inhibit cleavage of MICA/B off from the surface of HCT-116 cells. We found that both RDM028 and chimeric RDM028hG1, similar with the positive control antibody CLN-619 [23], markedly increased the surface expression of MICA and MICB on HCT-116 cells (Fig. 5D and E) resulting in decreased amounts of MICA in the cell culture supernatant from the cultured HCT-116 cells (Fig. 5F). These results suggest that RDM028 targets the site that is critical for the cleavage of MICA/B proteins.

4.3. Anti-tumor activity mediated by MICA/B α3 domain-specific antibody

To investigate whether augmentation of MICA/B proteins on cell surface will enhance the cytotoxicity of NK cells against tumor cells via MICA-NKG2D interactions, we conducted co-culture experiments with human HCT-116 and NK cells. For this purpose, HCT-116 cells were first treated with anti-MICA/B antibodies to inhibit release of MICA/B from the cell surface and then co-cultured with NK cells to evaluate the anti-tumor efficacy of NK cells. Our results demonstrated that both RDM028hG1 and CLN-619 significantly enhanced the NK cell-mediated killing of tumor cells, while RDM28 exhibited a noticeably weaker tumor-killing effect compared to CLN-619 (Fig. 6A). Furthermore, similar experimental results were obtained using another colon cancer cell line SW480 (Supplementary Fig. 3). In addition, we also examined the changes in the levels of the cytokine IFN-γ in the supernatant of HCT-116 cells co-cultured with NK cells after treatment with anti-MICA/B antibodies. The results showed a significant increase in the levels of IFN-γ in the supernatant of the cell cultures co-incubated with NK cells following treatment with RDM028, RDM028hG1 or CLN-619 antibodies (Supplementary Fig. 4). The increased amounts of these cytokines in the cell cutures were likely associated with the anti-tumor cytotoxicity. To evaluate if the tumor-suppressive effect of RDM028hG1 and RDM028 can be blunted upon blocking of the NKG2D receptor, NK cells were treated with the known NKG2D blocking antibody 1D11 [24]. We demonstrated that NKG2D blocking antibody 1D11 inhibited this effect (Fig. 6B). These findings indicated that the increased tumor-killing activity by NK cells was through the interaction of NKG2D with MICA as results from the increased surface expression of MICA/B.

Anti-tumor effect of MICA/B α3 domain-specific antibodies *in vivo* was evaluated next in a nude mouse xenograft tumor model

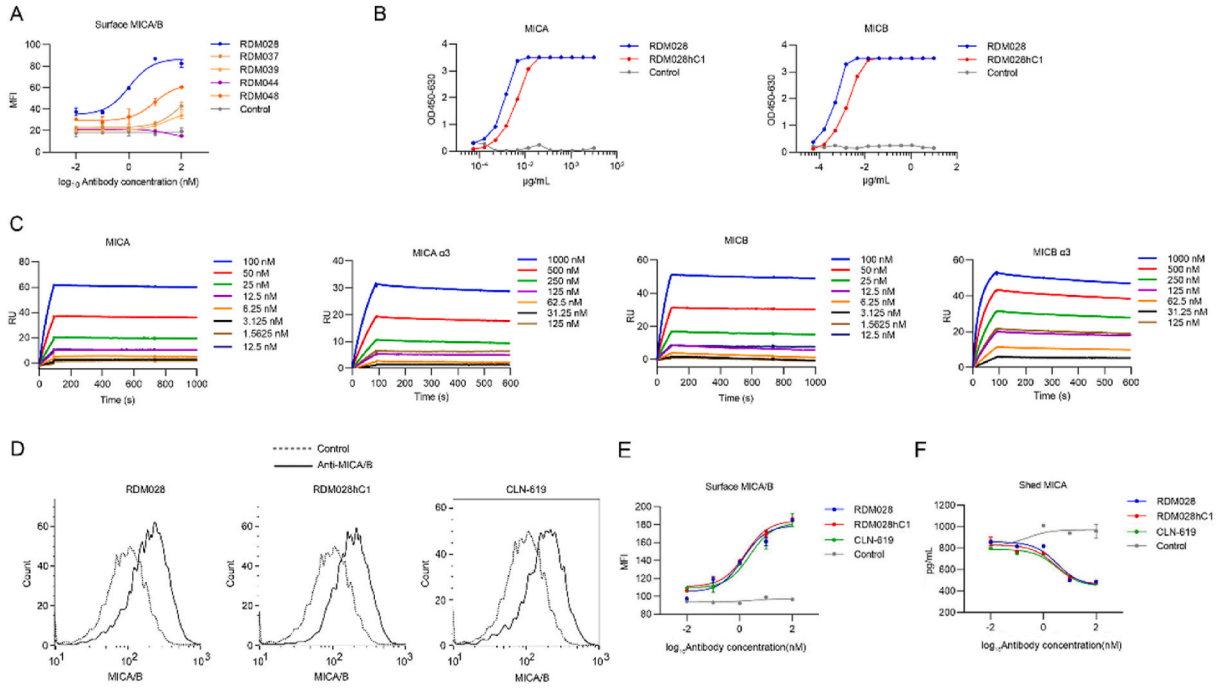

Fig. 5. Role of MICA/B-reactive mAbs on cell surface expression of MICA and MICAB. Surface expression (presented as mean fluorescence intensity analyzed by flow cytometric analysis at y axis) of MICA/B on HCT-116 cultured for 24 h in the presence of the indicated MICA/B-reactive mAbs at concentrations ranging from 0.01 nM to 100 nM at x axis (A). Comparison of RDM028 with chemeric RDM028hG1 to bind MICA and MICAB (B). Binding kinetics of RDM028hG1 chimeric antibody to MICA, MICB and their respective α3 structural domains measured by SPR (C). Surface expression of MICA/B on HCT-116 cells cultured for 24 h with MPE8 antibody (control), or in the presence of the indicated concentrations of RDM028,chemeric RDM028hG1, or the positive control antibody CLN-619 that was analyzed by flow cytometry and presented as flow cytometric graphs (D) or as fluorescence intensity plots (E). Soluble MICA/B proteins released in culture supernatant from the same HCT-116 cell cultures described in D were detected by ELISA (F).

using CC HTC-116 cells. Our findings demonstrated that injection of RDM028hG1 significantly suppressed tumor growth as decrease in tumor size (Fig. 6C and D) and tumor weight (Fig. 6E). In spite of no statistical significance in body weight change between the RDM028hG1-treated and control groups, mice treated with RDM028hG1 had higher body weight compared to the mice in negative control group. The lower body weight in the control group may be caused by decreased appetite or restricted movement due to tumor growth (Fig. 6F).

5. Discussion

Cancer immune surveillance is a vital host defense mechanism that effectively prevents the development of carcinogenesis and maintains cellular homeostasis. In particular, the importance of the interaction of NKG2D with its ligands MICA and MICB is strongly implicated in tumor immune surveillance [25]. Nevertheless, tumor cells have developed multiple mechanisms, such as reduction of the surface expression of NKG2D ligands by cleavage of MICA and MICB with matrix metalloproteinase (MMP)-929, MMP143, a disintegrin and metalloproteinase (ADAM)-9, ADAM10, ADAM17 and ERp5 thiol oxidoreductase, to evade NKG2D-mediated immune surveillance [26,27]. Since multiple enzymes can cleave MICA/B from the surface of tumor cells, it would not be effective for immunotheapy to develop a strategy by targeting the individual enzymes to mitigate shedding of MICA/B. Optimal strategies entail the utilization of antibodies to specifically target the enzymatic cleavage site on MICA/B proteins. It has been reported that inhibition of cleavage of MICA and MICB by α3 domain-specific antibody promotes NK-directed antibody-dependent cellular cytotoxicity and anti-tumor activity [9,17]. However, there are no reports on anti-tumor activity driven by MICA/B antibodies carried out for CC in animal study.

MAbs are an important tool in clinical and immunological research and play important roles in diagnosis and therapeutics. Many technologies have been developed to isolate mAbs from humans and immunized animals. Hybridoma, based on the fusion of B cells, is the most commonly used platform [28] but is inefficient and time-consuming [29]. In recent decades, *in vitro* display methodologies, including phage display [30], yeast surface display [31], ribosome display [32] and mRNA display, have been widely used for mAb isolation. Nonetheless, these techniques rely mostly on random combinations of the Ig heavy- and light-chain genes, leading to the loss of the original pairing information of antibodies. In recent years, there has been significant progress in developing a single B cell technology by combining of single B cell sorting and Ig gene amplification from single cells followed by *in vitro* production of re-combinant mAbs to reflect the native authentic antibodies using the isolated Ig genes to circumvent the inefficiency of hybridoma

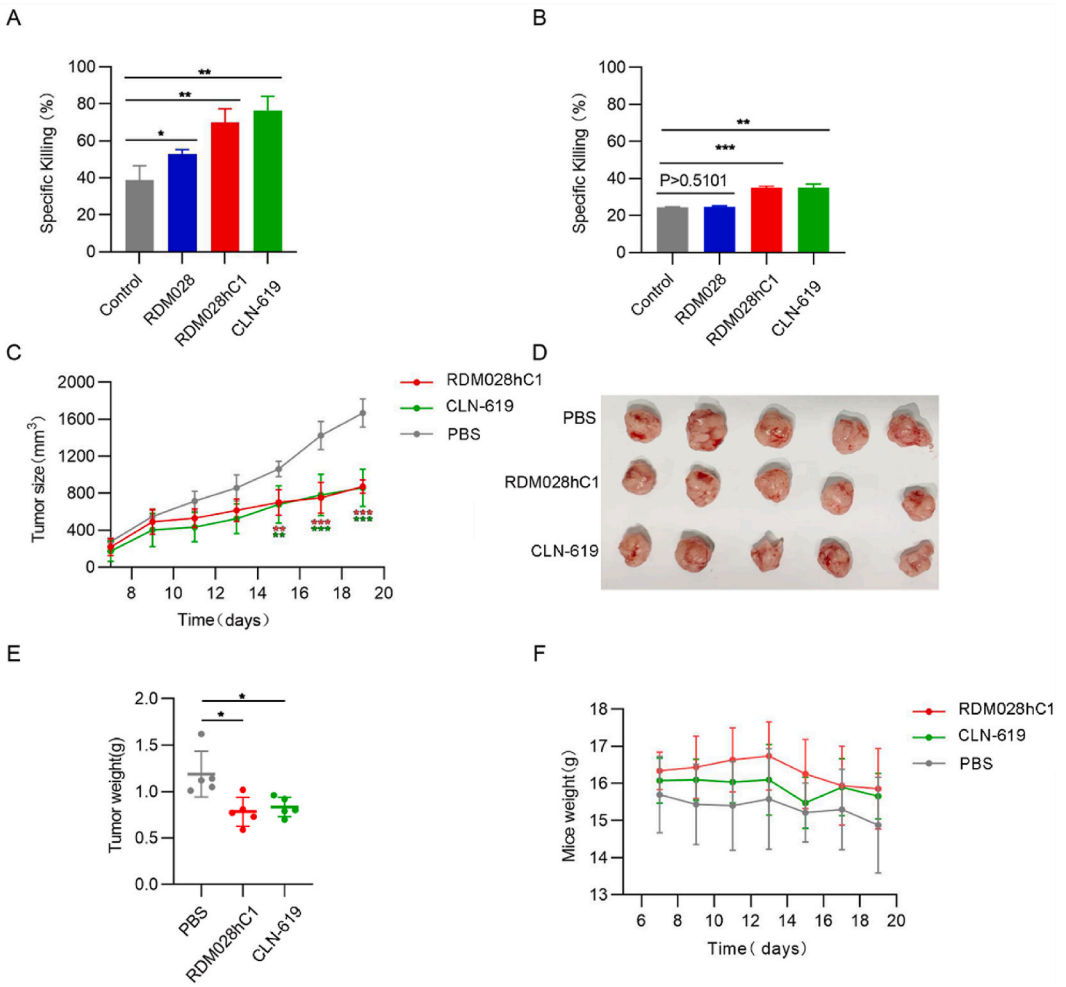

Fig. 6. Anti-tumor effects of the RDM028hG1 antibody in vitro and in vivo. Anti-tumor cytotoxicity mediated by RDM028, RDM028hG1 and the positive control antibody CLN619 were evaluated in HCT-116 cells in vitro without (A) or with (B) the presence of NKG2D receptor blocking antibody. (C–F) Analysis of the tumor-suppressive effect of RDM028hG1 in vivo. Tumor volume (C) and body weight (F) were measured every 2 days starting from day 7. Mice were euthanized when the tumor volume reached 2000 mm^3 (day 19). and the tumors were excised (D) and weighed (E). Results are presented as means ± standard deviations. Statistical analysis was performed using an unpaired *t*-test. $*p < 0.05$, $**p < 0.01$, $***p < 0.001$.

fusion and preserve the original heavy- and light-chain pairing and sequences. As a result, this technology has been successfully employed in isolation of wide specitrum of functional mAbs for rational design of structure-based vaccines, exploration of interaction of pathogens with host antibodies, mechanisms of pathogenesis, host immune responses and antibody theapeutics [33–35]. Moreover, this fast and efficient technique has become a very powerful approach for rapid isolation and development of mAbs from different animal species [36–40] and humans [20,41].

To explore the opportunity to use MICA/B antibodies as an anti-tumor therapeutic agent, we attempted to generate MICA/B antibodies in mice immunized with recombinant MICA/B proteins as immunogens and utilized successfully the single B cell technology for isolating a panel of MICA/B-specific mAbs. We have demonstrated that mAb RDM028 had strongest ability binding to a3 domain of bothMICA and MICB protein among the isolated 5 antibodies and had strongest ability augmenting the surface expression of MICA/B. The ability to increase the surface expression of MICA/B was likely due to blockage of cleavage of MICA/B since the increased surface expression of MICA/B was associated with the reduced levels of MICA/B detected from the culture supernantant of HCT0116 cell culture. Although the precise binding epitope and mechanism by which mAb RDM028 increased the surface expression of MICA/B remain to be elucidated, we believe that RDM028 must bind to a site on a3 domain that is critical for cleavage of MICA and MICB by enzymes.

Our study has confirmed that the RDM028hG1 antibody enhanced the interaction of MICA/B on the surface of colon cancer cells with NKG2D on the membrane of NK cells, resulting in potent anti-tumor cell cytotoxicity. Blockade of the NKG2D pathway with the 1D11 antibody did not completely abolish the NK cell-mediated killing effect through RDM028hG1. The reason for that is because the activation of NK cells to kill tumor cells involves not only the NKG2D pathway but also the activation of the CD16 Fc receptor.

Additionally, efficacy of RDM028 in killing tumor cells was not as strong as RDM028hG1, possibly due to the different effects of the CD16 Fc receptor activation mediated by the two antibodies. Thus, the anti-tumor effect of RDM028hG1 antibody in a nude mouse xenograft tumor model was likely through this mechanism. In spite of that HCT-116 is a human-derived cell line, these results are in consistent with the observation that human MICA/B proteins can be recognized by mouse NKG2D receptors in mice [17]. In addition, MICA/B antibodies could also induce ADCC to suppress tumor cells [42]. These findings offer a new avenue for study of anti-CC antibody therapy in nude mice as an *in vivo* xenograft model of CC.

As the first initial step toward a long-term goal to humanize RDM028 with the hope that RDM028 can eventually be developed as an anti-tumor therapeutic agent, RDM028 was produced as a chimeric antibody with the constant domain of human IgG1. The chimeric RDM028hG1 had binding profiles to MICA and MICB similar to that of RDM028. For eventual use of RDM028 as mouse-originated antibody as therapeutic agent, further extensive studies in humanization of the antibody will be needed to minimize the potential reactivity and immunogenicity in humans.

Taken together, this study provides additional data in supporting the role of antibodies targeting MICA/B to promote NK killing of tumors as an important strategy in anti-cancer immunotherapy.

Funding support

This research was mainly funded by the Zhuhai Trinomab Pharmaceutical Co. and supported partially by the Zhuhai Innovative and Entrepreneurial Research Team Program (grant number: 2120004000202) and the Zhuhai City Core Industries and Key Technology Research Directions Projects (grant number: 2220004002373).

Ethics approval and consent to participate

All of animal experiments in this study were carried under protocols approved by the Ethical Committee of Animal Experiments of Zhuhai BesTest Bio-Tech Co,.Ltd., ZhuHai, PR China (ethical permit IAC202301004).

Data availability statement

The data that support the findings of this study are available from the corresponding authors, Yayu Wang, Hua-Xin Liao and Yun Xia, upon reasonable request.

CRediT authorship contribution statement

Xueyi Tang: Writing – original draft, Methodology. **Linhai He:** Writing – original draft, Methodology. **Xiaoli Wang:** Methodology. **Shuaichao Liu:** Methodology. **Xiangning Liu:** Methodology. **Xiaorui Shen:** Methodology. **Yun Shu:** Methodology. **Ke Yang:** Methodology. **Qionghua Zhou:** Methodology. **Zujian Shan:** Methodology. **Yueming Wang:** Methodology. **Changwen Wu:** Methodology. **Zhenxing Jia:** Methodology. **Tong Liu:** Methodology. **Yayu Wang:** Writing – original draft, Methodology. **Hua-Xin Liao:** Writing – review & editing, Project administration, Funding acquisition. **Yun Xia:** Writing – review & editing, Supervision, Project administration.

Declaration of competing interest

Patent application by Trinomab for anti-MICA/B mAbs used in the study is pending. All authors declare no potential conflicts of interests.

Appendix A. Supplementary data

Supplementary data to this article can be found online at https://doi.org/10.1016/j.heliyon.2024.e35697.

References

[1] R. Siegel, K. Miller, H. Fuchs, A. Jemal, Cancer statistics, 2022, CA A Cancer J. Clin. 72 (1) (2022) 7–33, https://doi.org/10.3322/caac.21708. PubMed PMID: 35020204.

[2] C. Lichtenstern, R. Ngu, S. Shalapour, M. Karin, Immunotherapy, inflammation and colorectal cancer, Cells 9 (3) (2020), https://doi.org/10.3390/cells9030618. PubMed PMID: 32143413.

[3] A. Eggermont, C. Blank, M. Mandala, G. Long, V. Atkinson, S. Dalle, et al., Adjuvant pembrolizumab versus placebo in resected stage III melanoma, N. Engl. J. Med. 378 (19) (2018) 1789–1801, https://doi.org/10.1056/NEJMoa1802357. PubMed PMID: 29658430.

[4] L. Gandhi, D. Rodríguez-Abreu, S. Gadgeel, E. Esteban, E. Felip, F. De Angelis, et al., Pembrolizumab plus chemotherapy in metastatic non-small-cell lung cancer, N. Engl. J. Med. 378 (22) (2018) 2078–2092, https://doi.org/10.1056/NEJMoa1801005. PubMed PMID: 29658856.

[5] W. Hugo, J. Zaretsky, L. Sun, C. Song, B. Moreno, S. Hu-Lieskovan, et al., Genomic and transcriptomic features of response to anti-PD-1 therapy in metastatic melanoma, Cell 165 (1) (2016) 35–44, https://doi.org/10.1016/j.cell.2016.02.065. PubMed PMID: 26997480.

[6] J. Schachter, A. Ribas, G. Long, A. Arance, J. Grob, L. Mortier, et al., Pembrolizumab versus ipilimumab for advanced melanoma: final overall survival results of a multicentre, randomised, open-label phase 3 study (KEYNOTE-006), Lancet (London, England) 390 (10105) (2017) 1853–1862, https://doi.org/10.1016/s0140-6736(17)31601-x. PubMed PMID: 28822576.

[7] P. Dhar, J. Wu, NKG2D and its ligands in cancer, Curr. Opin. Immunol. 51 (2018) 55–61, https://doi.org/10.1016/j.coi.2018.02.004. PubMed PMID: 29525346.

[8] G. Chitadze, D. Kabelitz, Immune surveillance in glioblastoma: role of the NKG2D system and novel cell-based therapeutic approaches, Scand. J. Immunol. 96 (2) (2022) e13201, https://doi.org/10.1111/sji.13201. PubMed PMID: 35778892.

[9] C. Du, J. Bevers, R. Cook, T. Lombana, K. Rajasekaran, M. Matsumoto, et al., MICA immune complex formed with alpha 3 domain-specific antibody activates human NK cells in a Fc-dependent manner, Journal for immunotherapy of cancer 7 (1) (2019) 207, https://doi.org/10.1186/s40425-019-0687-9. PubMed PMID: 31387641.

[10] T. Lombana, M. Matsumoto, A. Berkley, E. Toy, R. Cook, Y. Gan, et al., High-resolution glycosylation site-engineering method identifies MICA epitope critical for shedding inhibition activity of anti-MICA antibodies, mAbs 11 (1) (2019) 75–93, https://doi.org/10.1080/19420862.2018.1532767. PubMed PMID: 30307368.

[11] V. Groh, S. Bahram, S. Bauer, A. Herman, M. Beauchamp, T. Spies, Cell stress-regulated human major histocompatibility complex class I gene expressed in gastrointestinal epithelium, Proc. Natl. Acad. Sci. U.S.A. 93 (22) (1996) 12445–12450, https://doi.org/10.1073/pnas.93.22.12445. PubMed PMID: 8901601.

[12] L. Pereboeva, L. Harkins, S. Wong, L. Lamb, The safety of allogeneic innate lymphocyte therapy for glioma patients with prior cranial irradiation, Cancer Immunol. Immunother. : CII. 64 (5) (2015) 551–562, https://doi.org/10.1007/s00262-015-1662-z. PubMed PMID: 25676710.

[13] L. Lamb, J. Bowersock, A. Dasgupta, G. Gillespie, Y. Su, A. Johnson, et al., Engineered drug resistant γδ T cells kill glioblastoma cell lines during a chemotherapy challenge: a strategy for combining chemo- and immunotherapy, PLoS One 8 (1) (2013) e51805, https://doi.org/10.1371/journal.pone.0051805. PubMed PMID: 23326319.

[14] E. Doubrovina, M. Doubrovin, E. Vider, R. Sisson, R. O'Reilly, B. Dupont, et al., Evasion from NK cell immunity by MHC class I chain-related molecules expressing colon adenocarcinoma, Journal of immunology (Baltimore, Md : 1950) 171 (12) (2003) 6891–6899, https://doi.org/10.4049/jimmunol.171.12.6891. PubMed PMID: 14662896.

[15] B. Kaiser, D. Yim, I. Chow, S. Gonzalez, Z. Dai, H. Mann, et al., Disulphide-isomerase-enabled shedding of tumour-associated NKG2D ligands, Nature 447 (7143) (2007) 482–486, https://doi.org/10.1038/nature05768. PubMed PMID: 17495932.

[16] H. Salih, H. Rammensee, A. Steinle, Cutting edge: down-regulation of MICA on human tumors by proteolytic shedding, Journal of immunology (Baltimore, Md : 1950) 169 (8) (2002) 4098–4102, https://doi.org/10.4049/jimmunol.169.8.4098. PubMed PMID: 12370336.

[17] L. Ferrari de Andrade, R. Tay, D. Pan, A. Luoma, Y. Ito, S. Badrinath, et al., Antibody-mediated inhibition of MICA and MICB shedding promotes NK cell-driven tumor immunity, Science (New York, NY) 359 (6383) (2018) 1537–1542, https://doi.org/10.1126/science.aao0505. PubMed PMID: 29599246.

[18] T. Courau, J. Bonnereau, J. Chicoteau, H. Bottois, R. Remark, L. Assante Miranda, et al., Cocultures of human colorectal tumor spheroids with immune cells reveal the therapeutic potential of MICA/B and NKG2A targeting for cancer treatment, Journal for immunotherapy of cancer 7 (1) (2019) 74, https://doi.org/10.1186/s40425-019-0553-9. PubMed PMID: 30871626.

[19] G. Haughton, L. Lanier, G. Babcock, The murine kappa light chain shift, Nature 275 (5676) (1978) 154–157, https://doi.org/10.1038/275154a0. PubMed PMID: 99664.

[20] H. Liao, M. Levesque, A. Nagel, A. Dixon, R. Zhang, E. Walter, et al., High-throughput isolation of immunoglobulin genes from single human B cells and expression as monoclonal antibodies, J. Virol Methods 158 (2009) 171–179, https://doi.org/10.1016/j.jviromet.2009.02.014. PubMed PMID: 19428587.

[21] Y. Wang, C. Wu, J. Yu, S. Lin, T. Liu, L. Zan, et al., Structural basis of tetanus toxin neutralization by native human monoclonal antibodies, Cell Rep. 35 (5) (2021) 109070, https://doi.org/10.1016/j.celrep.2021.109070. PubMed PMID: 33951441.

[22] X. Wang, A. Lundgren, P. Singh, D. Goodlett, S. Plymate, J. Wu, An six-amino acid motif in the alpha3 domain of MICA is the cancer therapeutic target to inhibit shedding, Biochem. Biophys. Res. Commun. 387 (3) (2009) 476–481, https://doi.org/10.1016/j.bbrc.2009.07.062. PubMed PMID: 19615970.

[23] K.A. Whalen, N.K. Mehta, S. Yalcin, K. Meetze, N.W. Gibson, J.S. Michaelson, et al. (Eds.), CLN-619, a Clinical-Stage MICA/MICB-specific IgG1 Antibody, Restores the MICA/MICB-NKG2D axis to Promote NK-Mediated Tumor Cell Lysis, AMER ASSOC CANCER RESEARCH 615 CHESTNUT ST, 17TH FLOOR, Cancer Research, PHILADELPHIA, PA, 2022.

[24] G. Chitadze, M. Lettau, C. Peters, S. Luecke, C. Flüh, E. Quabius, et al., Erroneous expression of NKG2D on granulocytes detected by phycoerythrin-conjugated clone 149810 antibody, Cytometry B Clin. Cytometry 102 (3) (2022) 228–238, https://doi.org/10.1002/cyto.b.22001. PubMed PMID: 33749106.

[25] M. Qian, J. Geng, K. Luo, Z. Huang, Q. Zhang, J. Zhang, et al., BCL11B regulates MICA/B-mediated immune response by acting as a competitive endogenous RNA, Oncogene 39 (7) (2020) 1514–1526, https://doi.org/10.1038/s41388-019-1083-0. PubMed PMID: 31673069.

[26] G. Chitadze, M. Lettau, J. Bhat, D. Wesch, A. Steinle, D. Fürst, et al., Shedding of endogenous MHC class I-related chain molecules A and B from different human tumor entities: heterogeneous involvement of the "a disintegrin and metalloproteases" 10 and 17, Int. J. Cancer 133 (7) (2013) 1557–1566, https://doi.org/10.1002/ijc.28174. PubMed PMID: 23526433.

[27] Y. Morimoto, N. Yamashita, T. Daimon, H. Hirose, S. Yamano, N. Haratake, et al., MUC1-C is a master regulator of MICA/B NKG2D ligand and exosome secretion in human cancer cells, Journal for immunotherapy of cancer 11 (2) (2023), https://doi.org/10.1136/jitc-2022-006238. PubMed PMID: 36754452.

[28] G. Köhler, C. Milstein, Continuous cultures of fused cells secreting antibody of predefined specificity, Nature 256 (5517) (1975) 495–497, https://doi.org/10.1038/256495a0. PubMed PMID: 1172191.

[29] Z. Zhang, H. Liu, Q. Guan, L. Wang, H. Yuan, Advances in the isolation of specific monoclonal rabbit antibodies, Front. Immunol. 8 (2017) 494, https://doi.org/10.3389/fimmu.2017.00494. PubMed PMID: 28529510.

[30] G. Smith, Filamentous fusion phage: novel expression vectors that display cloned antigens on the virion surface, Science (New York, NY) 228 (4705) (1985) 1315–1317, https://doi.org/10.1126/science.4001944. PubMed PMID: 4001944.

[31] T. Murai, M. Ueda, M. Yamamura, H. Atomi, Y. Shibasaki, N. Kamasawa, et al., Construction of a starch-utilizing yeast by cell surface engineering, Appl. Environ. Microbiol. 63 (4) (1997) 1362–1366, https://doi.org/10.1128/aem.63.4.1362-1366.1997. PubMed PMID: 9097432.

[32] J. Hanes, L. Jermutus, S. Weber-Bornhauser, H. Bosshard, A. Plückthun, Ribosome display efficiently selects and evolves high-affinity antibodies in vitro from immune libraries, Proc. Natl. Acad. Sci. U.S.A. 95 (24) (1998) 14130–14135, https://doi.org/10.1073/pnas.95.24.14130. PubMed PMID: 9826665.

[33] J. Wrammert, K. Smith, J. Miller, W. Langley, K. Kokko, C. Larsen, et al., Rapid cloning of high-affinity human monoclonal antibodies against influenza virus, Nature 453 (7195) (2008) 667–671, https://doi.org/10.1038/nature06890. PubMed PMID: 18449194.

[34] L. Morris, X. Chen, M. Alam, G. Tomaras, R. Zhang, D. Marshall, et al., Isolation of a human anti-HIV gp41 membrane proximal region neutralizing antibody by antigen-specific single B cell sorting, PLoS One 6 (9) (2011) e23532, https://doi.org/10.1371/journal.pone.0023532. PubMed PMID: 21980336.

[35] H. Liao, R. Lynch, T. Zhou, F. Gao, S. Alam, S. Boyd, et al., Co-evolution of a broadly neutralizing HIV-1 antibody and founder virus, Nature 496 (7446) (2013) 469–476, https://doi.org/10.1038/nature12053. PubMed PMID: 23552890.

[36] J. Rashidian, J. Lloyd, Single B cell cloning and production of rabbit monoclonal antibodies, Methods Mol. Biol. 2070 (2020) 423–441, https://doi.org/10.1007/978-1-4939-9853-1_23. PubMed PMID: 31625109.

[37] R. Zhang, D. Martinez, Q. Nguyen, J. Pollara, T. Arifin, C. Stolarchuk, et al., Envelope-specific B-cell populations in African green monkeys chronically infected with simian immunodeficiency virus, Nat. Commun. 7 (2016) 12131, https://doi.org/10.1038/ncomms12131. PubMed PMID: 27381634.

[38] D. Starkie, J. Compson, S. Rapecki, D. Lightwood, Generation of recombinant monoclonal antibodies from immunised mice and rabbits via flow cytometry and sorting of antigen-specific IgG+ memory B cells, PLoS One 11 (3) (2016) e0152282, https://doi.org/10.1371/journal.pone.0152282. PubMed PMID: 27022949.

[39] T. Tiller, C. Busse, H. Wardemann, Cloning and expression of murine Ig genes from single B cells, J. Immunol. Methods 350 (2009) 183–193, https://doi.org/10.1016/j.jim.2009.08.009. PubMed PMID: 19716372.

[40] N. Kurosawa, M. Yoshioka, R. Fujimoto, F. Yamagishi, M. Isobe, Rapid production of antigen-specific monoclonal antibodies from a variety of animals, BMC Biol. 10 (2012) 80, https://doi.org/10.1186/1741-7007-10-80. PubMed PMID: 23017270.

[41] K. Smith, L. Garman, J. Wrammert, N. Zheng, J. Capra, R. Ahmed, et al., Rapid generation of fully human monoclonal antibodies specific to a vaccinating antigen, Nat. Protoc. 4 (3) (2009) 372–384, https://doi.org/10.1038/nprot.2009.3. PubMed PMID: 19247287.

[42] J.D. Powderly, M. Gutierrez, J.S. Wang, E.P. Hamilton, M. Sharma, A.I. Spira, et al., A phase 1 dose-escalation study to investigate the safety, efficacy, pharmacokinetics, and pharmacodynamic activity of CLN-619. (anti-MICA/MICB Antibody) Alone and in Combination with Pembrolizumab in Patients with Advanced Solid Tumors, American Society of Clinical Oncology, 2022.